Activation thresholds in epidemic spreading with motile infectious agents on scale-free networks

Cite as: Chaos **28**, 123112 (2018); https://doi.org/10.1063/1.5050807
Submitted: 02 August 2018 . Accepted: 08 November 2018 . Published Online: 10 December 2018

Diogo H. Silva, and Silvio C. Ferreira

Activation thresholds in epidemic spreading with motile infectious agents on scale-free networks

Diogo H. Silva[1] and Silvio C. Ferreira[1,2]
[1]*Departamento de Física, Universidade Federal de Viçosa, 36570-900 Viçosa, Minas Gerais, Brazil*
[2]*National Institute of Science and Technology for Complex Systems, 22290-180, Rio de Janeiro, Brazil*

(Received 2 August 2018; accepted 8 November 2018; published online 10 December 2018)

We investigate a fermionic susceptible-infected-susceptible model with the mobility of infected individuals on uncorrelated scale-free networks with power-law degree distributions $P(k) \sim k^{-\gamma}$ of exponents $2 < \gamma < 3$. Two diffusive processes with diffusion rate D of an infected vertex are considered. In the *standard diffusion*, one of the nearest-neighbors is chosen with equal chance, while in the *biased diffusion*, this choice happens with probability proportional to the neighbor's degree. A non-monotonic dependence of the epidemic threshold on D with an optimum diffusion rate D_*, for which the epidemic spreading is more efficient, is found for standard diffusion while monotonic decays are observed in the biased case. The epidemic thresholds go to zero as the network size is increased and the form that this happens depends on the diffusion rule and the degree exponent. We analytically investigated the dynamics using quenched and heterogeneous mean-field theories. The former presents, in general, a better performance for standard and the latter for biased diffusion models, indicating different activation mechanisms of the epidemic phases that are rationalized in terms of hubs or max k-core subgraphs. *Published by AIP Publishing.* https://doi.org/10.1063/1.5050807

Nowadays, we live in an interwoven world where information, goods, and people move through a complex structure with widely diversified types of interactions such as on-line friendship and airport connections. These and many other systems of completely distinct nature can be equally suited in a theoretical representation called complex networks, in which the elements are represented by vertices and the interactions among them by edges connecting these vertices. The study of epidemic processes on complex networks represents one of the cornerstones in modern network science and can aid the prevention (or even stimulation) of disease or misinformation spreading. The relevance of the interplay between diffusion and epidemic spreading in real systems is self-evident since hosts of infectious agents, such as people and mobile devices, are constantly moving, being the carriers that promote the quick transition from a localized outbreak to a large scale epidemic scenario. In this work, we perform a theoretical analysis and report nontrivial roles played by mobility of infected agents on the efficiency of epidemic spreading running on the top of complex networks. We expect that our results will render impacts for forthcoming research related to the area.

I. INTRODUCTION

Any system that allows an abstract mathematical representation where the vertices are elements connected by edges representing interactions among them can be suited in the complex network framework.[1] A network can be characterized by several statistical properties such as the degree distribution probability $P(k)$ that a randomly selected vertex has k contacts (k is called vertex degree). Many real networks such as Internet,[2] actor and scientific collaboration,[3] and airport connections[4,5] possess degree distributions with power-law tails in the form[1] $P(k) \sim k^{-\gamma}$.

The importance of dynamics processes taking place on the top of a network are on an equal footing as its structural properties.[6] The simplest example is a standard random walk, in which a particle lying on the vertices of the network hops to a nearest-neighbor randomly selected. For connected undirected networks, the stationary probability to find a walker on a vertex is proportional to its degree.[7] Since a random walk is a very basic search mechanism, a deeper understanding of this dynamical process can aid the building of efficient strategies to find a specific content in a network.[8] Moreover, the patterns of mobility of individuals is an issue of increasing relevance that nowadays can be experimentally tracked back using bluetooth and Internet,[9] mobile phones,[10] or radio-frequency identification devices.[11,12] Another important class of dynamic processes on networks is the epidemic spreading.[13] It is a remarkable example where an academic problem in complex systems has turned into applications in real processes as the forecast of outbreaks of Ebola,[14] H1N5 influenza,[15] and Zika virus[16] to mention only a few examples. A kind of epidemic spreading whose importance has increased significantly is the virus dissemination in mobile devices.[17]

Relevance of the interplay between diffusion and epidemic spreading in real systems is self-evident since hosts of infectious agents, such as people and mobile devices, are constantly moving and being the carriers that promote the quick transition from a localized outbreak to a large scale epidemics.[4,5,15] Diffusion has been investigated on networks for *bosonic* epidemic processes where the vertices can be simultaneously occupied by several individuals[18] and, in particular, within the context of heterogeneous metapopulations,[19–23] where each vertex consists itself of a subpopulation and the edges represent possibility of

interchange of individuals moving from one subpopulation to another according to a mobility rule. When infected and healthy individuals move with the same rate on a metapopulation, the concentration of both types is proportional to the vertex degree.[20] On lattices, diffusion in bosonic models can lead to complex outcomes such as discontinuous or continuous absorbing-state phase transitions depending on the diffusion rates of infected and susceptible (that can be infected) individuals.[24]

Epidemic process is commonly investigated within a *fermionic* approach, in which each vertex can host a single individual.[13] Mean-field theories predict equivalent critical properties and evolution for bosonic and fermionic reaction-diffusion processes but they are not identical.[18] One fundamental epidemic process with a stationary active state is the susceptible-infected-susceptible (SIS) model,[13] where the vertices can be in one of the two states: susceptible, which can be infected, and infected that can transmit the infection. Infected individuals become spontaneously susceptible with rate μ, while the susceptible ones in contact with z infected individuals are infected with rate λz. Despite its simplicity, the SIS model on networks with power-law degree distributions presents complex behaviors and has been the subject of intensive research.[13,25] Some important features of the SIS model have been discussed in its fermionic version as, for example, the value of the epidemic threshold above which the epidemics lasts forever in the thermodynamical limit,[26] how this limit is approached,[27–30] and the localization of the epidemic activity.[31–36]

The epidemic threshold of the SIS model on random graphs with power-law degree distribution is null in the thermodynamical limit,[26] irrespective of the degree exponent γ. The epidemic threshold of the SIS model is commonly investigated using mean-field methods.[13] Two basic ones are the heterogeneous mean-field (HMF) [2] and quenched mean-field (QMF)[37] theories. Recent reviews can be found elsewhere.[13,25] The former considers a compartmental approach where vertices with the same degree have the same chance to be infected while the latter takes into account the actual structure of network through its adjacency matrix; see Sec. III. The QMF theory is able to capture the asymptotic null threshold analytically expected[26] and observed in simulations[27] for all values of $\gamma > 2$, while the zero threshold happens only for $2 < \gamma < 3$ in HMF.

In this paper, we investigate a diffusive fermionic SIS model where infected agents hop to their nearest neighbors with rate D. Two rules, with (*biased diffusion*) and without (*standard diffusion*) tendency to higher degree vertices, are investigated. We observe that moderate diffusion enhances epidemic activity in hubs and the threshold asymptotically vanishes for both models while the finite-size scaling of the threshold depends strongly on the diffusion model and the degree exponent of the networks. For a fixed size, the standard diffusion model presents an optimum value of D, in which the epidemic threshold is minimal while a monotonic decay is found for biased diffusion. Comparisons between HMF and QMF theories with the thresholds obtained in simulations on scale-free networks with $\gamma < 3$ show, in general, a higher accuracy of QMF for standard and HMF for biased diffusion models indicating different activation mechanisms[39,40] for these mobility strategies.

The remaining of the paper is organized as follows. In Sec. II, we define the diffusive SIS models, briefly review and present the properties of random walks on networks for the investigated mobility rules. The mean-field equations and their stability analyses are presented in Sec. III. The numerical methods are presented in Sec. IV. Simulations are compared with the mean-field theories in Sec. V. The implications and interpretations of the results are presented in Sec. VI. We summarize our conclusions and prospects in Sec. VII.

II. MODELS

The models consist of the SIS dynamics described in Sec. I with rates λ and μ on a network of N vertices, including diffusion of infected individuals with rate D. The healing rate is fixed as $\mu = 1$ without loss of generality. Diffusion consists of the exchange of states between the infected vertex and one of its nearest-neighbors selected according to a given rule. It worths to stress that the exchange between two infected vertices does not lead to a new state. The absence of diffusion of the susceptible vertices is motivated by simplification of the computer implementation of the stochastic simulations.

We investigated two diffusion rules. In the standard diffusion, the state of an infected vertex i of degree k_i is exchanged with a randomly selected nearest-neighbor j such that the exchange rate from vertex i to j is

$$D_{ij} = \frac{DA_{ij}}{k_i}, \tag{1}$$

where D is the diffusion coefficient and A_{ij} is the adjacency matrix defined as $A_{ij} = 1$ if i and j are connected and $A_{ij} = 0$ otherwise. In the biased diffusion, the exchange is done preferentially with higher degree neighbors. Considering a simple linear relation $D_{ij} \propto A_{ij}k_j$, it can be written as

$$D_{ij} = \frac{DA_{ij}k_j}{k_i\bar{\kappa}_i}, \tag{2}$$

where

$$\bar{\kappa}_i = \frac{1}{k_i}\sum_j A_{ij}k_j \tag{3}$$

is the average degree of the nearest-neighbors of vertex i. This rule can represent, for example, the mobility pattern of people linked with the place where they live or work.[9] Both models obey the condition $\sum_j D_{ij} = D$.

The standard diffusion of a single random walker was solved[7] and the stationary probability that the walker is on a given vertex is proportional to its degree. Thus, one expects that diffusion will increase the concentration of infected individual on hubs. In the limit $D \to \infty$, the infected walker will visit essentially the entire network implying in high mixing where a mean-field regime is expected.

The random walk problem for biased diffusion on uncorrelated network with degree distribution $P(k)$ can be solved using the HMF theory. Let W_k be the probability that the

walker is at a vertex of degree k that evolves as

$$\frac{dW_k}{dt} = -DW_k + k\sum_{k'} P(k'|k)D_{k'k}W_{k'}, \tag{4}$$

where $D_{k'k} = Dk/[k'\bar{\kappa}(k)]$ is the diffusion rate from a vertex of degree k' to a vertex of degree k and $P(k'|k)$ is the probability that a vertex of degree k is connected to a vertex of degree k'. Assuming the absence of degree correlations, we have[41] $P(k'|k) = k'P(k')/\langle k\rangle$ and $\bar{\kappa}(k) = \langle k^2\rangle/\langle k\rangle$. In the stationary state, the probability of finding a walker on a vertex of degree k is

$$W_k = \frac{k^2}{\langle k^2\rangle}, \tag{5}$$

where $\sum_k W_k P(k) = 1$ since the walker must be somewhere on the network. This result indicates a stronger trend to move to the most connected vertices in comparison with the standard diffusion.

III. MEAN-FIELD ANALYSIS

A. HMF theory

Let ρ_k be the density of infected vertices having degree k. Dynamic equations for this quantity are obtained including the diffusive terms in the HMF equations of the original SIS model[2] and become

$$\begin{aligned}\frac{d\rho_k}{dt} = &-\rho_k + \lambda k(1-\rho_k)\sum_{k'} P(k'|k)\rho_{k'} \\ &- k\rho_k\sum_{k'}(1-\rho_{k'})D_{kk'}P(k'|k) \\ &+ k(1-\rho_k)\sum_{k'} D_{k'k}P(k'|k)\rho_{k'}.\end{aligned} \tag{6}$$

The first and second terms on the right-hand side represent the healing and infection, respectively. The third and fourth terms correspond to the diffusion of infected vertices from or to a vertex of degree k, respectively, reckoning the contribution of vertices with different degrees.

For standard diffusion, we have $D_{kk'} = D/k$. Performing a linear stability analysis of the fixed point $\rho_k = 0$, we obtain the Jacobian matrix $J_{kk'} = -(1+D)\delta_{kk'} + C_{kk'}$, where

$$C_{kk'} = \left(\lambda + \frac{D}{k'}\right)kP(k'|k). \tag{7}$$

The epidemic threshold is obtained when the largest eigenvalue of the Jacobian matrix is zero. Assuming that the network is uncorrelated, we have that $C_{kk'}$ has a positive eigenvector $u_k = k$ with associated eigenvalue

$$\Lambda_1 = \lambda\frac{\langle k\rangle}{\langle k^2\rangle} + D. \tag{8}$$

Since $C_{kk'}$ is irreducible, the Perron-Frobenius theorem[42] guaranties that it is the largest eigenvalue. Thus, the epidemic threshold is

$$\lambda_c = \frac{\langle k\rangle}{\langle k^2\rangle}. \tag{9}$$

This expression is exactly the same found for the HMF theory of the non-diffusive SIS dynamics[2] and does not depend on the diffusion coefficient D. The threshold vanishes for $2 < \gamma < 3$ and is finite if $\gamma > 3$ as the network size $N \to \infty$.

Considering the biased diffusion with $D_{kk'} = Dk'/[k\bar{\kappa}(k)]$ and uncorrelated networks, the Jacobian matrix is

$$J_{kk'} = -(1+D)\delta_{kk'} + \frac{Dk^2P(k')}{\langle k^2\rangle} + \lambda\frac{kk'P(k')}{\langle k\rangle}. \tag{10}$$

We did not find a closed expression for the largest eigenvalue of this Jacobian and analyzed it using numerical diagonalization.[43]

B. QMF theory

Let ρ_i be the probability that the vertex i is infected. The QMF equation is also obtained introducing the diffusion terms in the non-diffusive equation[32] and it becomes

$$\begin{aligned}\frac{d\rho_i}{dt} = &-\rho_i + \lambda(1-\rho_i)\sum_j A_{ij}\rho_j \\ &- \rho_i\sum_j D_{ij}(1-\rho_j) + (1-\rho_i)\sum_j D_{ji}\rho_j.\end{aligned} \tag{11}$$

The meaning of each term is analogous to those of Eq. (6).

Linear stability analysis around $\rho_i = 0$ provides Jacobian matrix

$$J_{ij} = -(1+D)\delta_{ij} + \lambda A_{ij} + D_{ji}, \tag{12}$$

where D_{ij} is given by Eqs. (1) and (2) for standard and biased diffusion, respectively. Note that it is a general result regardless of the correlation patterns. The largest eigenvalues of the Jacobians and thus the epidemic thresholds are, in general, obtained with numerical diagonalization[43] unless for simple graphs as the one discussed in Subsection III C.

C. QMF theory for a leaking star graph

Due to its importance to understand the activation of epidemic processes with localized activity and, in particular, the SIS dynamics on networks,[26,28,29] we consider a star graph where the center, $i = 0$, is connected to K leaves, $i = 1, 2, \ldots, K$. To include the effects of the diffusion outwards the star, we assume that each leaf has degree $k_{\text{leaf}} = \langle k\rangle$ to mimic a hub in a network. These edges change the diffusion rate D_{10} from a leaf to the center ($D_{j0} = D_{10}$ for $j = 2, \ldots, K$) and permit that infected individuals in the leaves leak with rate $D_\varnothing$. Diffusion and infection from outside are disregarded. Due to the symmetry, we have that $\rho_1 = \rho_2 = \cdots \rho_K$ and the $K+1$ equations are reduced to a two-dimensional system

$$\begin{aligned}\frac{d\rho_0}{dt} = &-\rho_0 + \lambda K\rho_1(1-\rho_0) - D_{01}K\rho_0(1-\rho_1) \\ &+ D_{10}K\rho_1(1-\rho_0),\end{aligned} \tag{13}$$

$$\begin{aligned}\frac{d\rho_1}{dt} = &-\rho_1 + \lambda\rho_0(1-\rho_1) - D_{10}\rho_1(1-\rho_0) \\ &+ D_{01}\rho_0(1-\rho_1) - D_\varnothing\rho_1.\end{aligned} \tag{14}$$

A linear stability analysis around $\rho_i = 0$ provides the Jacobian

$$\mathbb{J} = \begin{bmatrix} -(1+D_{01}K) & (\lambda + D_{10})K \\ (\lambda + D_{01}) & -(1+D_{10}+D_\varnothing)\end{bmatrix}. \tag{15}$$

For standard diffusion, we have $D_{01} = D/K$, $D_{10} = D/\langle k\rangle$, and $D_{\varnothing} = (\langle k\rangle - 1)D/\langle k\rangle$ and setting the largest eigenvalue of the Jacobian to be zero we obtain an epidemic threshold

$$\lambda_c = \frac{D(K+\langle k\rangle)}{2K\langle k\rangle}\left[\sqrt{1+4K\langle k\rangle\frac{\langle k\rangle(1+D)^2 - D^2}{D^2(\langle k\rangle + K)^2}} - 1\right]. \tag{16}$$

Note that for $D \to 0$ and $K \gg \langle k\rangle$, we recover the known result for the QMF theory of non-diffusive SIS on a star graph[27] $\lambda_c \simeq 1/\sqrt{K}$. For $K \gg \langle k\rangle$, which represents hubs, and D finite we obtain

$$\lambda_c \simeq \frac{\langle k\rangle(1+D)^2 - D^2}{DK}. \tag{17}$$

The analysis is very similar for biased diffusion with the only differences that $D_{10} = DK/[K + \langle k\rangle(\langle k\rangle - 1))] \simeq D$ and $D_{\varnothing} = \langle k\rangle(\langle k\rangle - 1)/[K + \langle k\rangle(\langle k\rangle - 1)]$, in which we assume that all vertices outside the star have degree $\langle k\rangle$. The threshold for large K becomes

$$\lambda_c = \frac{D(K+1)}{2K}\left[\sqrt{1+4K\frac{2D+1}{D^2(K+1)^2}} - 1\right]. \tag{18}$$

For $K \gg \langle k\rangle$ and D finite, Eq. (18) yields

$$\lambda_c \simeq \frac{2D+1}{DK}. \tag{19}$$

Observe that the threshold for standard diffusion presents a minimum at

$$D_* \simeq \sqrt{\frac{\langle k\rangle}{\langle k\rangle - 1}}, \tag{20}$$

while in biased diffusion it varies monotonically with D. These behaviors are confirmed in simulations (see Sec. IV for algorithms and methods) on leaking star graphs shown in Fig. 1.

Taking the steady state of Eqs. (13) and (14), we obtain the density of infected vertices above the epidemic threshold

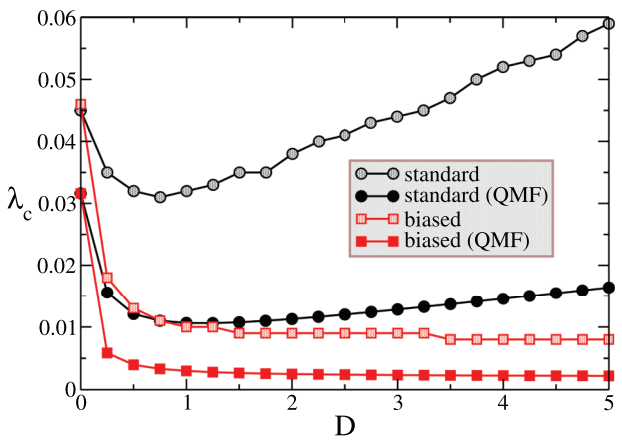

FIG. 1. Epidemic threshold for SIS with standard and biased diffusion on a leaking star graph obtained in QMF theory, Eqs. (16) and (18), and simulations, Sec. IV. A center with $K = 1000$ leaves and each leaf with $\langle k\rangle = 3$ neighbors were used.

for large K as

$$\rho = \frac{\lambda - \lambda_c}{1 + \lambda + \frac{\langle k\rangle - 1}{\langle k\rangle}D} \tag{21}$$

and

$$\rho = \frac{\lambda - \lambda_c}{1+\lambda} \tag{22}$$

for standard and biased diffusion, respectively. In both cases, a standard mean-field phase transition is obtained for $K \gg 1$, where $\rho \sim (\lambda - \lambda_c)^{\beta}$ with $\beta = 1$ is the same exponent of the non-diffusive case. Exploiting these expression further for λ slightly above λ_c, say $\lambda = a\lambda_c$ with $a \gtrsim 1$, we have that $\rho \sim 1/K$. These behaviors are very well fitted by stochastic simulations (data not shown).

IV. NUMERICAL METHODS

We investigated the SIS dynamics on leaking star graphs defined in Subsection III C and uncorrelated networks of size N with power-law degree distributions $P(k) \sim k^{-\gamma}$. The latter was generated with the uncorrelated configuration model (UCM)[44] using lower and upper degree cutoffs $k_{\min} = 3$ and $k_{\max} = \sqrt{N}$, respectively, granting the absence of the degree correlations in the scale-free regime with $2 < \gamma < 3$.

The algorithm to simulate the SIS model with diffusion is based on the optimized Gillespie algorithms with phantom processes[45] that do not imply in changes of configurations but count for time increments. Let N_{inf} be the number of infected vertices and N_{e} the sum of the degree of all infected vertices. In each time step, one of the following three events is tried. (i) With probability

$$P_{\text{heal}} = \frac{\mu N_{\text{inf}}}{(\mu + D)N_{\text{inf}} + \lambda N_{\text{e}}}, \tag{23}$$

a randomly selected vertex is spontaneously healed. (ii) With probability

$$P_{\text{inf}} = \frac{\lambda N_{\text{e}}}{(\mu + D)N_{\text{inf}} + \lambda N_{\text{e}}}, \tag{24}$$

one infected vertex is chosen with probability proportional to its degree and one of its nearest-neighbors is selected with equal chance. If the neighbor is susceptible it becomes infected. (iii) Finally, with probability

$$P_{\text{dif}} = \frac{DN_{\text{inf}}}{(\mu + D)N_{\text{inf}} + \lambda N_{\text{e}}}, \tag{25}$$

the states of an infected vertex and one of its nearest-neighbors are exchanged. The target neighbor is chosen with equal chance in standard diffusion and with a probability proportional to its degree in biased diffusion. The time is incremented by $dt = -\ln(u)/[(\mu + D)N_{\text{inf}} + \lambda N_{\text{e}}]$, where u is a pseudo-random number uniformly distributed in the interval $(0, 1)$, while N_{inf} and N_{e} are updated accordingly.

We apply the standard quasistationary method,[46] in which the dynamics is reactivated to some previously visited configuration, to deal with the absorbing state with $N_{\text{inf}} = 0$ in a finite size system near to the transition point. Implementation details can be found elsewhere.[45,47] The quasistationary probability $\bar{P}_n$ that the system has n infected vertices near the transition is computed over a time interval $t_{\text{av}} = 10^7$ after

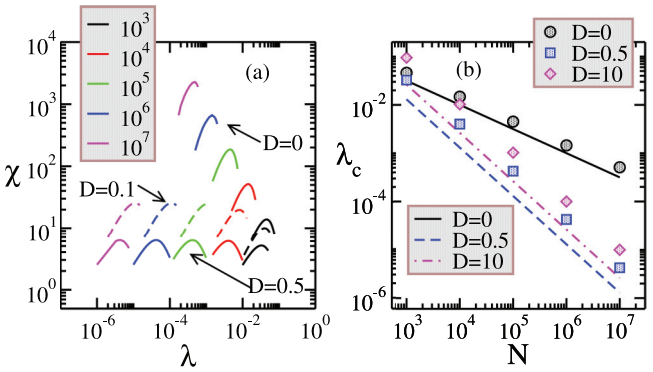

FIG. 2. (a) Susceptibility as a function of the infection rate for leaking star graphs of different sizes (shown in the legends) with $\langle k\rangle = 3$. The cases without diffusion, $D = 0$, and with small standard diffusion rates, $D = 0.1$ (dashed lines) and 0.5, are shown. (b) Threshold as a function of the network size for different values of D obtained with simulations (symbols) and QMF theory (lines).

a relaxation time $t_{\rm rlx} = 10^6$. Larger or smaller values were used for very subcritical and supercritical simulations, respectively. We analyze the quasistationary density $\langle\rho\rangle$, which is the order parameter that defines active and inactive phases, and the dynamical susceptibility[27]

$$\chi = N\frac{\langle\rho^2\rangle - \langle\rho\rangle^2}{\langle\rho\rangle}, \tag{26}$$

whose the position of the maximum yields the effective (size-dependent) epidemic threshold.

V. THEORY VS SIMULATIONS

In this section, we compare the thresholds obtained in the mean-field theories with quasistationary simulations. Rigorously, for a finite system the unique asymptotic stationary state is the absorbing one where all vertices are susceptible.[38] In this work, we deal with an effective finite-size threshold above which the epidemic lifespan becomes extremely large.

A. Leaking star graphs

The QMF predictions given by Eqs. (16) and (18) are compared with simulations on leaking star graphs in Figs. 1 and 2. We see that the theory correctly predicts the qualitative dependence on D for a fixed size, Fig. 1, as well as the scaling of the threshold as a function of the size, Fig. 2(b), regardless of $D > 0$. The dynamical susceptibility at the transition diverges as the network size increases in agreement with a critical transition[48] without diffusion[27,49] while it saturates in the presence of diffusion irrespective of the value of D if the graph size is sufficiently large. These behaviors of the susceptibility and scaling of the threshold are observed in the biased diffusion model too (data not shown). The saturation happens because the center is reinfected almost instantaneously after it becomes susceptible since the total diffusion rate to the center is proportional to $N_{\rm inf}D \gg 1$, where $N_{\rm inf}$ is the number of infected leaves. The center constantly infected depletes fluctuations in the number of infected individuals that determines the order parameter.

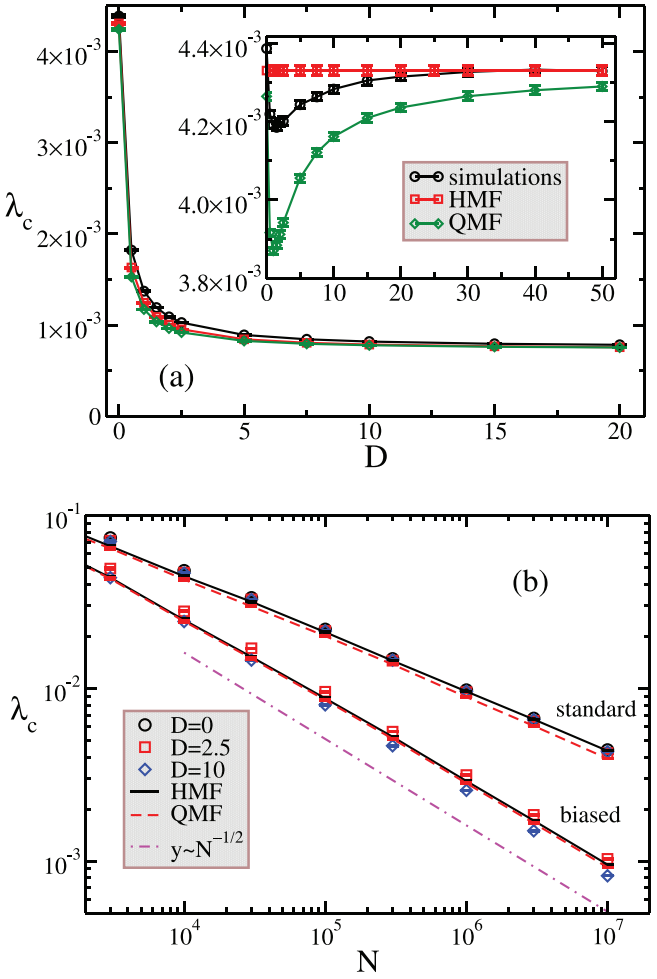

FIG. 3. Epidemic thresholds for the diffusive SIS models on UCM networks with degree exponent $\gamma = 2.25$. (a) Dependence with diffusion rate for a network of size $N = 10^7$. Main panel shows biased while the inset shows standard diffusion models. (b) Finite-size analysis of the epidemic threshold for both diffusion models. The scaling predicted for a star subgraph with $K = k_{\rm max} \simeq \sqrt{N}$, $\lambda_c^{\rm (star)} \sim N^{-1/2}$, is also shown.

B. Power-law networks with $2 < \gamma < 2.5$

We compare the epidemic thresholds of simulations for UCM networks with $\gamma = 2.25$ with mean-field theories for both diffusion models in Fig. 3. The curves show a dependence with the diffusion coefficient D qualitatively described by QMF but quantitatively better fitted by the HMF theory. Observe the narrow scale for the threshold variation in the standard diffusion in the inset of Fig. 3(a). We observe a quantitative good agreement between simulations and HMF and QMF theories in both models, which is evident in the finite-size analysis shown in Fig. 3(b). The standard diffusion presents scaling with size in agreement with the HMF theory given by $\lambda_c^{\rm (HMF)} = \langle k\rangle/\langle k^2\rangle \sim {k_{\rm max}}^{\gamma-3} \sim N^{-0.375}$ for $\gamma = 2.25$. The scaling for biased diffusion is also captured by the HMF theory but it additionally coincides with the QMF theory with the same scaling of a leaking star subgraph centered on the most connected vertex that scales as $\lambda_c^{\rm (star)} \sim {k_{\rm max}}^{-1} \sim N^{-1/2}$.

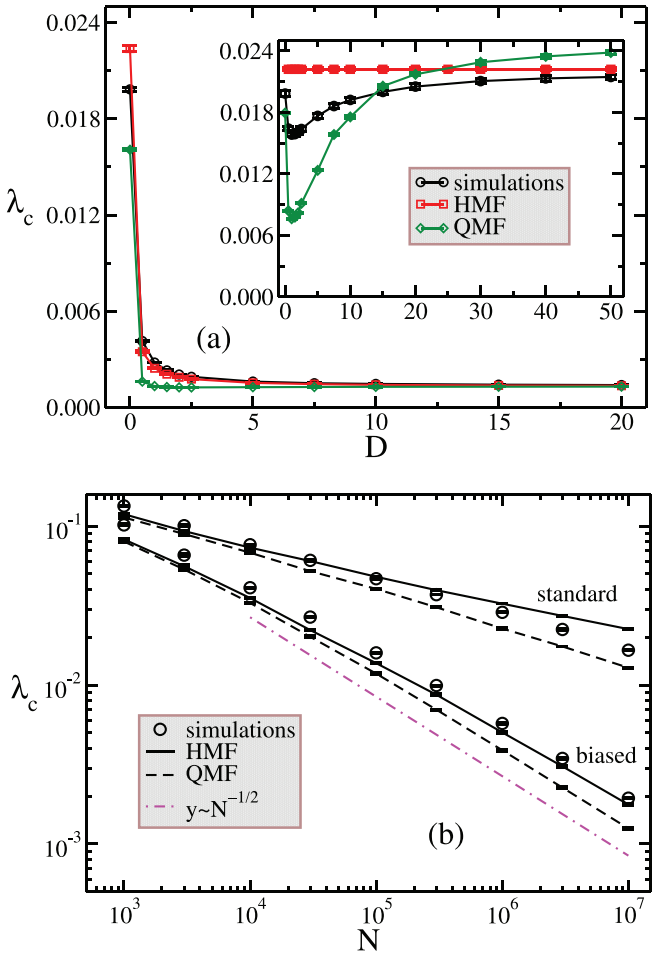

FIG. 4. Epidemic thresholds for the diffusive SIS model on UCM networks with degree exponent $\gamma = 2.75$. (a) Dependence with the diffusion rate for a network of size $N = 10^7$. The main panel shows biased while the inset standard diffusion models. (b) Finite-size analysis of the epidemic threshold for both diffusion models with $D = 2.5$. The scaling predicted for the epidemic threshold on a leaking star graph with $K = k_{\max} \simeq \sqrt{N}$, $\lambda_c^{(\text{star})} \sim N^{-1/2}$, is also shown.

C. Power-law networks with $2.5 < \gamma < 3$

The curves $\lambda_c(D)$ for UCM networks with fixed size $N = 10^7$ and exponent $\gamma = 2.75$ are shown in Fig. 4(a). The qualitative picture observed for $\gamma < 2.5$ does not change with the presence of an optimum value where the threshold is minimum in the case of standard diffusion. Quantitatively, a considerably larger variability of the threshold as a function of D is found for standard diffusion. Another difference for large D is that QMF deviates from both the HMF theory and simulations. The last two converge to each other. Theory performances for standard and biased diffusions can be seen in the finite-size analysis of the threshold for a fixed diffusion coefficient in Fig. 4(b). While standard diffusion is quantitatively better fitted by the QMF than the HMF theory, as in the non-diffusive case,[27,49] the biased diffusion is clearly better described by the HMF theory, which predicts accurately both scaling and amplitude of the epidemic threshold as a function of the size. Within the investigated size range, the threshold decay in the QMF theory for the biased diffusion asymptotically scales as that of a leaking star subgraph centered on the most connected vertex with degree $K \simeq \sqrt{N}$, $\lambda_c^{(\text{star})} \sim N^{-1/2}$, but this was not observed for standard diffusion.

VI. DISCUSSION

We start our discussion with the epidemic threshold dependence on the diffusion coefficient D for a fixed network size. The non-monotonic dependence on D for the standard and the monotonic decay for biased diffusion models regardless of the degree exponent γ seems to be reminiscent of the hub activation since they qualitatively agree with the threshold obtained for leaking star graph shown in Fig. 1 and are qualitatively captured by the QMF theory. The role played by diffusion in the activation of hubs is stronger in the biased case, as initially suggested by the analysis of random walks in Sec. II, in which a much stronger tendency to move toward hubs is found with biased diffusion. Despite the different thresholds, both dynamics are well described by the HMF theory in the high diffusion limit, which is expected since high mobility promotes mixing and breaks down pairwise dynamical correlations. In such a regime, HMF theory becomes exact in the thermodynamical limit.

The finite-size scaling of the epidemic threshold in a size range $10^3 < N < 10^7$ shows further differences with respect to the performance of the mean-field theories. For $\gamma < 2.5$, both QMF and HMF theories have good performance for both models. However, for $2.5 < \gamma < 3$, the standard diffusion is better described by QMF, while HMF presents a much better performance for biased diffusion.

Two different mechanisms have been associated to the activation of the epidemics in the non-diffusive SIS model on uncorrelated scale-free networks.[39] A discussion for a more general epidemics can be found elsewhere.[50] For $\gamma < 2.5$, the epidemics in SIS is triggered in a densely connected component of the network identified by the maximum index of a k-core decomposition, hereafter called as max k-core.[55] For $\gamma > 2.5$ this activation is triggered in the largest hubs of the network. The epidemic process with max k-core activation mechanism was well described by a HMF theory, which is an intrinsically collective theory due to its close relation with annealed networks,[52] while the hub mechanism is better suited within a QMF theory involving a few elements of the network, namely, the hubs. This conjecture relating activation mechanisms and suitability of mean-field theories has been verified for other epidemic models.[40,53] Applying this conjecture to the diffusive SIS models, we have that the activation happens in the max k-core for the biased diffusion in the whole range $2 < \gamma < 3$ and the same scheme of the non-diffusive SIS is valid for the standard diffusion, with hub triggering activation for $\gamma > 2.5$ and max k-core for $\gamma < 2.5$. Table I summarizes the distinct frameworks observed in our analysis of the diffusive SIS models with respect to the most suitable mean-field theory and the triggering activation mechanisms in each case.

We could naturally wonder why do biased and standard diffusion models behave so differently if mobility favors localization in hubs for both cases? A high diffusivity implies that the infected individual stays shortly in a same vertex. In standard diffusion, when the infected individual leaves a hub toward a randomly selected neighbor, it more probably

TABLE I. Schematic summary of the basic properties of diffusive SIS models for two regimes of scale-free networks.

Model	$2 < \gamma < 2.5$	$2.5 < \gamma < 3$
Standard	HMF and QMF work max k-core activation	QMF outperforms HMF hub activation
Biased	HMF and QMF work max k-core activation	HMF outperforms QMF max k-core activation

arrives at a low degree vertex, present in a much larger number, where it spreads the infection less efficiently. So, even enhancing mobility to higher degree vertices, the net effect of sufficiently high standard diffusion is to reduce the infection power of hubs. In the biased diffusion, the mobility toward hubs is highly favored such that the infected individual stays moving mostly among hubs keeping, therefore, its spreading efficiency at high levels. Moreover, these high degree vertices belong to the max k-core in random scale-free networks in consonance with the activation mechanism for $2.5 < \gamma < 3$ in the biased diffusion model.

VII. CONCLUDING REMARKS

Mobility is a fundamental promoter of epidemic spreading in real world and its effects on epidemic models on networks have been dealt in the context of bosonic processes, where a single vertex can host several infected individuals.[20] A lot of theoretical attention has been dedicated to the investigation of fermionic epidemic models where no more than one individual can lay on a vertex.[13] However, the effects of mobility in the fermionic epidemic models on networks have been not addressed thoroughly. We consider the role played by mobility in the phase transition of two fermionic diffusive SIS models on scale-free networks with degree distribution $P(k) \sim k^{-\gamma}$ and exponent $2 < \gamma < 3$. Both standard and biased diffusion models were considered. In the latter, higher degree vertices are favored.

The epidemic thresholds were investigated on large networks using stochastic simulations and compared with QMF and HMF theories. Biases reduce significantly the epidemic threshold for a fixed network size, and is very well described by the HMF theory. Standard diffusion yields a non-monotonic dependence on D with an optimum value D_*, where the threshold at a given size is minimum. The QMF theory describes better the epidemic threshold for standard diffusion. Different triggering mechanisms of the epidemic phase were identified. While biased diffusion leads to a max k-core activation for all values of $2 < \gamma < 3$, the standard diffusion behaves as the non-diffusive case, being activated by hubs for $\gamma > 2.5$ and max k-core for $\gamma < 2.5$.

Outstanding examples of theoretical studies for epidemic process on networks[2,13] currently guide applied research in predicting real-world epidemic outbreaks. Therefore, understanding better the role of mobility in epidemic processes can aid the improvement and accuracy of these realistic models. Our study reveals non-trivial effects of the mobility on the outcomes of epidemic models running on the top of heterogeneous networks. We expect that it will render impacts for forthcoming research in the field. As prospects, the case $\gamma > 3$ needs further attention. Our first analysis points out a very strong depletion of the fluctuations, markedly changing the nature of the epidemic transition. Still, from the application point of view, the role of correlation and assortativity patterns, which are ubiquitous in real networked systems, as well as the mobility of susceptible individuals also need additional investigations. Finally, the inclusion of dynamical correlations using heterogeneous pairwise approximations[49,54] can provide more accurate predictions in forthcoming studies.

ACKNOWLEDGMENTS

This work was partially supported by the Brazilian agencies CAPES, CNPq and FAPEMIG. S.C.F. thanks the support from the program *Ciência sem Fronteiras*—CAPES under Project No. 88881.030375/2013-01. This study was financed in part by the Coordenação de Aperfeiçoamento de Pessoal de Nível Superior - Brasil (CAPES) - Finance Code 001.

[1] A.-L. Barabási and M. Pósfai, *Network Science* (Cambridge University Press, Cambridge, 2016).
[2] R. Pastor-Satorras, A. Vázquez, and A. Vespignani, "Dynamical and correlation properties of the internet," Phys. Rev. Lett. **87**, 258701 (2001).
[3] J. J. Ramasco, S. N. Dorogovtsev, and R. Pastor-Satorras, "Self-organization of collaboration networks," Phys. Rev. E **70**, 036106 (2004).
[4] V. Colizza, A. Barrat, M. Barthelemy, and A. Vespignani, "The role of the airline transportation network in the prediction and predictability of global epidemics," Proc. Natl. Acad. Sci. **103**, 2015–2020 (2006).
[5] A. Vespignani, "Modelling dynamical processes in complex socio-technical systems," Nat. Phys. **8**, 32–39 (2012).
[6] A. Barrat, M. Barthelemy, and A. Vespignani, *Dynamical Processes on Complex Networks* (Cambridge University Press, Cambridge, 2008).
[7] J. D. Noh and H. Rieger, "Random walks on complex networks," Phys. Rev. Lett. **92**, 118701 (2004).
[8] N. Masuda, M. A. Porter, and R. Lambiotte, "Random walks and diffusion on networks," Phys. Rep. **716–717**, 1–58 (2017).
[9] N. Eagle and A. Pentland, "Reality mining: Sensing complex social systems," Pers. Ubiquitous Comput. **10**, 255–268 (2006).
[10] M. C. González, C. A. Hidalgo, and A.-L. Barabási, "Understanding individual human mobility patterns," Nature **453**, 779–782 (2008).
[11] C. Cattuto, W. Van den Broeck, A. Barrat, V. Colizza, J.-F. Pinton, and A. Vespignani, "Dynamics of person-to-person interactions from distributed RFID sensor networks," PLoS One **5**, e11596 (2010).
[12] J. Stehlé, N. Voirin, A. Barrat, C. Cattuto, L. Isella, J.-F. Pinton, M. Quaggiotto, W. Van den Broeck, C. Régis, B. Lina, and P. Vanhems, "High-resolution measurements of face-to-face contact patterns in a primary school," PLoS One **6**, e23176 (2011).
[13] R. Pastor-Satorras, C. Castellano, P. Van Mieghem, and A. Vespignani, "Epidemic processes in complex networks," Rev. Mod. Phys. **87**, 925–979 (2015).
[14] M. F. C. Gomes, A. Pastore y Piotti, L. Rossi, D. Chao, I. Longini, and M. E. Halloran, "Assessing the international spreading risk associated with the 2014 west african ebola outbreak," PLoS Curr. **19**, 1–22 (2014).
[15] V. Colizza, A. Barrat, M. Barthelemy, A.-J. Valleron, and A. Vespignani, "Modeling the worldwide spread of pandemic influenza: Baseline case and containment interventions," PLoS Med. **4**, e13 (2007).
[16] Q. Zhang, K. Sun, M. Chinazzi, A. Pastore y Piontti, N. E. Dean, D. P. Rojas, S. Merler, D. Mistry, P. Poletti, L. Rossi, M. Bray, M. E. Halloran, I. M. Longini, and A. Vespignani, "Spread of Zika virus in the Americas," Proc. Natl. Acad. Sci. **114**, E4334–E4343 (2017).
[17] P. Wang, M. C. Gonzalez, C. A. Hidalgo, and A.-L. Barabasi, "Understanding the spreading patterns of mobile phone viruses," Science **324**, 1071–1076 (2009).
[18] A. Baronchelli, M. Catanzaro, and R. Pastor-Satorras, "Bosonic reaction-diffusion processes on scale-free networks," Phys. Rev. E **78**, 016111 (2008).
[19] M. J. Keeling and C. A. Gilligan, "Metapopulation dynamics of bubonic plague," Nature **407**, 903–906 (2000).

[20]V. Colizza, R. Pastor-Satorras, and A. Vespignani, "Reaction-diffusion processes and metapopulation models in heterogeneous networks," Nat. Phys. **3**, 276–282 (2007).
[21]V. Colizza and A. Vespignani, "Invasion threshold in heterogeneous metapopulation networks," Phys. Rev. Lett. **99**, 148701 (2007).
[22]A. S. Mata, S. C. Ferreira, and R. Pastor-Satorras, "Effects of local population structure in a reaction-diffusion model of a contact process on metapopulation networks," Phys. Rev. E **88**, 042820 (2013).
[23]J. Gómez-Gardeñes, D. Soriano-Paños, and A. Arenas, "Critical regimes driven by recurrent mobility patterns of reaction-diffusion processes in networks," Nat. Phys. **14**, 391–395 (2018).
[24]D. S. Maia and R. Dickman, "Diffusive epidemic process: Theory and simulation," J. Phys. Condens. Matter **19**, 065143 (2007).
[25]W. Wang, M. Tang, H. Eugene Stanley, and L. A. Braunstein, "Unification of theoretical approaches for epidemic spreading on complex networks," Rep. Prog. Phys. **80**, 036603 (2017).
[26]S. Chatterjee and R. Durrett, "Contact processes on random graphs with power law degree distributions have critical value 0," Ann. Probab. **37**, 2332–2356 (2009).
[27]S. C. Ferreira, C. Castellano, and R. Pastor-Satorras, "Epidemic thresholds of the susceptible-infected-susceptible model on networks: A comparison of numerical and theoretical results," Phys. Rev. E **86**, 041125 (2012).
[28]C. Castellano and R. Pastor-Satorras, "Thresholds for epidemic spreading in networks," Phys. Rev. Lett. **105**, 218701 (2010).
[29]M. Boguñá, C. Castellano, and R. Pastor-Satorras, "Nature of the epidemic threshold for the susceptible-infected-susceptible dynamics in networks," Phys. Rev. Lett. **111**, 068701 (2013).
[30]C.-R. Cai, Z.-X. Wu, M. Z. Q. Chen, P. Holme, and J.-Y. Guan, "Solving the dynamic correlation problem of the susceptible-infected-susceptible model on networks," Phys. Rev. Lett. **116**, 258301 (2016).
[31]A. S. Mata and S. C. Ferreira, "Multiple transitions of the susceptible-infected-susceptible epidemic model on complex networks," Phys. Rev. E **91**, 012816 (2015).
[32]A. V. Goltsev, S. N. Dorogovtsev, J. G. Oliveira, and J. F. F. Mendes, "Localization and spreading of diseases in complex networks," Phys. Rev. Lett. **109**, 128702 (2012).
[33]H. K. Lee, P.-S. Shim, and J. D. Noh, "Epidemic threshold of the susceptible-infected-susceptible model on complex networks," Phys. Rev. E **87**, 062812 (2013).
[34]G. St-Onge, J.-G. Young, E. Laurence, C. Murphy, and L. J. Dubé, "Phase transition of the susceptible-infected-susceptible dynamics on time-varying configuration model networks," Phys. Rev. E **97**, 022305 (2018).
[35]G. Ódor, "Spectral analysis and slow spreading dynamics on complex networks," Phys. Rev. E **88**, 32109 (2013).
[36]W. Cota, S. C. Ferreira, and G. Ódor, "Griffiths effects of the susceptible-infected-susceptible epidemic model on random power-law networks," Phys. Rev. E **93**, 032322 (2016).
[37]D. Chakrabarti, Y. Wang, C. Wang, J. Leskovec, and C. Faloutsos, "Epidemic thresholds in real networks," ACM Trans. Inf. Syst. Secur. **10**, 1:1–1:26 (2008).
[38]J. Marro and R. Dickman, *Nonequilibrium Phase Transitions in Lattice Models* (Cambridge University Press, Cambridge, 2005).
[39]C. Castellano and R. Pastor-Satorras, "Competing activation mechanisms in epidemics on networks," Sci. Rep. **2**, 371 (2012).
[40]W. Cota, A. S. Mata, and S. C. Ferreira, "Robustness and fragility of the susceptible-infected-susceptible epidemic models on complex networks," Phys. Rev. E **98**, 012310 (2018).
[41]M. Boguñá and R. Pastor-Satorras, "Class of correlated random networks with hidden variables," Phys. Rev. E **68**, 036112 (2003).
[42]M. Newman, *Networks: An Introduction* (OUP Oxford, 2010).
[43]W. H. Press, *Numerical Recipes* (Cambridge University Press, Cambridge, 2007).
[44]M. Catanzaro, M. Boguñá, and R. Pastor-Satorras, "Generation of uncorrelated random scale-free networks," Phys. Rev. E **71**, 027103 (2005).
[45]W. Cota and S. C. Ferreira, "Optimized gillespie algorithms for the simulation of markovian epidemic processes on large and heterogeneous networks," Comput. Phys. Commun. **219**, 303–312 (2017).
[46]M. M. de Oliveira and R. Dickman, "How to simulate the quasistationary state," Phys. Rev. E **71**, 016129 (2005).
[47]R. S. Sander, G. S. Costa, and S. C. Ferreira, "Sampling methods for the quasistationary regime of epidemic processes on regular and complex networks," Phys. Rev. E **94**, 042308 (2016).
[48]U. C. Tauber, *Critical Dynamics* (Cambridge University Press, Cambridge, 2014).
[49]A. S. Mata and S. C. Ferreira, "Pair quenched mean-field theory for the susceptible-infected-susceptible model on complex networks," Europhys. Lett. **103**, 48003 (2013).
[50]M. Kitsak, L. K. Gallos, S. Havlin, F. Liljeros, L. Muchnik, H. E. Stanley, and H. A. Makse, "Identification of influential spreaders in complex networks," Nat. Phys. **6**, 888–893 (2010).
[51]S. N. Dorogovtsev, A. V. Goltsev, and J. F. F. Mendes, "*k*-core organization of complex networks," Phys. Rev. Lett. **96**, 040601 (2006).
[52]M. Boguñá, C. Castellano, and R. Pastor-Satorras, "Langevin approach for the dynamics of the contact process on annealed scale-free networks," Phys. Rev. E **79**, 036110 (2009).
[53]S. C. S. Ferreira, R. R. S. Sander, and R. Pastor-Satorras, "Collective versus hub activation of epidemic phases on networks," Phys. Rev. E **93**, 032314 (2016).
[54]A. S. Mata, R. S. Ferreira, and S. C. Ferreira, "Heterogeneous pair-approximation for the contact process on complex networks," New J. Phys. **16**, 053006 (2014).
[55]A k-core decomposition[51] consists of a pruning process that starts removing all vertices with degree $k_s = k_{\min}$ plus their edges and any other vertex whose degree became $k_{\min}$ after the removal, until no more vertices of degree $k_{\min}$ are present. The procedure is sequentially repeated for $k_s = k_{\min} + 1$, $k_{\min} + 2$ and so on until all vertices are removed. The max k-core corresponds to the subset of vertices and edges removed in the last step of the decomposition.